

Theddeus Tochukwu Akano ¹, Patrick Shola Olayiwola¹

Nonlinear mechanics of a compliant beam system undergoing large curvature deformation

A compliant beam subjected to large deformation is governed by a multifaceted nonlinear differential equation. In the context of theoretical mechanics, solution for such equations plays an important role. Since it is hard to find closed-form solutions for this nonlinear problem and attempt at direct solution results in linearising the model. This paper investigates the aforementioned problem via the multi-step differential transformation method (MsDTM), which is well-known approximate analytical solutions. The nonlinear governing equation is established based on a large radius of curvature that gives rise to curvature-moment nonlinearity. Based on established boundary conditions, solutions are sort to address the free vibration and static response of the deforming flexible beam. The geometrically linear and nonlinear theory approaches are related. The efficacy of the MsDTM is verified by a couple of physically related parameters for this investigation. The findings demonstrate that this approach is highly efficient and easy to determine the solution of such problems. In new engineering subjects, it is forecast that MsDTM will find wide use.

1. Introduction

This paper presents a theoretical model of the nonlinear behaviour of compliant beams. A compliant mechanism (CM) is a mechanism that derives any or more of its movement from the deformation of slender segments rather than from the relative movement of coupled joints along rigid-body connections [1]. The nonlinear behaviour of this type of structure is postulated to come from its ability to undergo large deformation at minimum load. The nonlinear equations must be derived and measured numerically and analytically to verify this assertion.

✉ Theddeus Tochukwu Akano, e-mail: takano@unilag.edu.ng

¹University of Lagos, Lagos, Nigeria; e-mail: psolayiwola@unilag.edu.ng



Many investigations on the topic of nonlinear beam deformation have been published. From its chronological order of investigation, we have a look at some concise works on this subject matter. For the geometrically nonlinear broad elastic beam deflection, Bishop and Drucker [2] presented a classic mathematical approach with a vertical edge load. Many researchers who follow thereafter leveraged on their theoretical solution, to proffer answers to many unresolved questions. Starting with Wang [3, 4] who suggested numerical methods for the study of nonlinear beam bending under a tip and uniformly distributed loads; to others like Sokolnikoff [5], Frisch-Fay [6], Gere and Timoshenko [7] and Howell [8] worked on the deformation of elastic problem in their respective prominent books; to Belendez et al. [9, 10] who elaborated the mathematical solution for ease of understanding and experimental extension. Other researchers [11–14] employed elliptical integrals or Jacobi elliptical functions to solve related problems in closed form. Equally based on the work of Bishop and Drucker [2], Zakharov and Okhotkin [15] and Batista [16] gave analytical solutions for equilibrium configurations of a cantilever rod subjected to inclined force and moment acting on its free end. Kumar et al. [17] suggested genetic search approaches based on algorithms for direct numerical solutions for differential equation control and applied the stationary principle of the balanced energy features. Dado and Al-Sadder [18] developed an approach that approximated the rotational angle of a polynomial function and used it effectively with a very large deflection for complex loads on an unprismatic beam. The large deflections of a cantilever beam subjected to a follower force was studied by Shvartsman [19], and extended by Mutyalarao et al. [20] to the uniqueness of the large deflection under tip rotational load. Rahman et al. [21] carried out nonlinear geometric analysis of parabolic leaf spring, while Roy and Saha [22] provided a nonlinear analysis of this leaf springs using variational method to find its deflection profiles. Banerjee et al. [23] proposed nonlinear shooting, combined with domain decomposition methods to determine the large deflection of a cantilever beam under arbitrary loading conditions. Chen [24] proposed an integral approach for large deflection study of a cantilever beam with complex load and varying beam properties. Large deflection of beams made of functionally graded material had been studied by different numerical approaches [25–27]. While Ghuku and Saha [28] conducted an experimental and theoretical analysis on the large deflection behaviour of initially curved beams, with different loading. More recently, studies into the nonlinear bending theory of fully nonlinear beams response are still ongoing [29, 30] to the investigation into the large deformation of the continuum compliant beam under point load [31].

Most theoretical problems in solid mechanics are essentially nonlinear by definition, and most of them have no empirical solutions except for a small number of cases. Nonlinear calculations are also typically resolved by using certain approaches for instance computational techniques or analytical methods. An analytical method that have been commonly used recently is one of the easy and

accurate approaches to solve the nonlinear differential equations. Sequentially, the differential transformation method (DTM) has been applied as an applicable analytical method. The DTM is based on the Taylor expansion. It constructs an analytical solution in the form of a polynomial. It is different from the traditional high order Taylor series method, which requires the symbolic computation of the necessary derivatives of the data functions. This method was first applied in the engineering domain by Zhou [32], and its abilities have attracted many authors to use this method for solving nonlinear equations. This scheme has successfully been applied to a couple of works [33–38]. For both linear and nonlinear equations, DTM has proven to be an efficient and convenient process; as it does not depend on a small parameter.

This article is intended to show that a compliant beam's nonlinear nature is because of the large deformation term. Therefore, large deformations must be generated if nonlinear definitions are to be used. To achieve this, MsDTM is deployed to analytically obtain the free vibration and static response of a flexible beam subjected transverse distributed load. MsDTM technique introduces an alternative framework designed to overcome the difficulty of capturing the periodic behaviour of the solution and give a good approximation to the true solution in a very large region. The effectiveness of MsDTM for this type of problem is tested through the results of a couple of physically relevant parameters studied.

The remainder of this article is structured accordingly. Section 2 explains how to use the nonlinear moment-curvature equation for large beam deflection as a derivation of the fundamental model. Section 3 provides the semi-analytical technique used for the solution of the nonlinear equation. Section 4 presents the analytical solution of the model for free vibration and the quasi-static response of the loaded beam. In section 7, the results and findings are eventually addressed. While section 8 ultimately provides the conclusion.

2. Nonlinear mechanics of the flexible beam

The selection of an effective mathematical model is the first stage of any analysis. This model needs to be formulated based on the analysis questions imposed. The selection of the geometry, material properties, the loading, boundary conditions, and any other specific assumptions made are sacrosanct to the model formulation. The study aims to address some questions concerning the structure's stiffness, stresses formed and strength. Therefore, when analysing the structure's behaviour, we would like to forecast the future, not just when the system operates under normal conditions, which often involves only a linear analysis, but also under extreme loading conditions, which typically involves a highly nonlinear analysis. Here, we will consider a compliant beam that undergoes large deformation using the deformed beam element in Fig. 1.

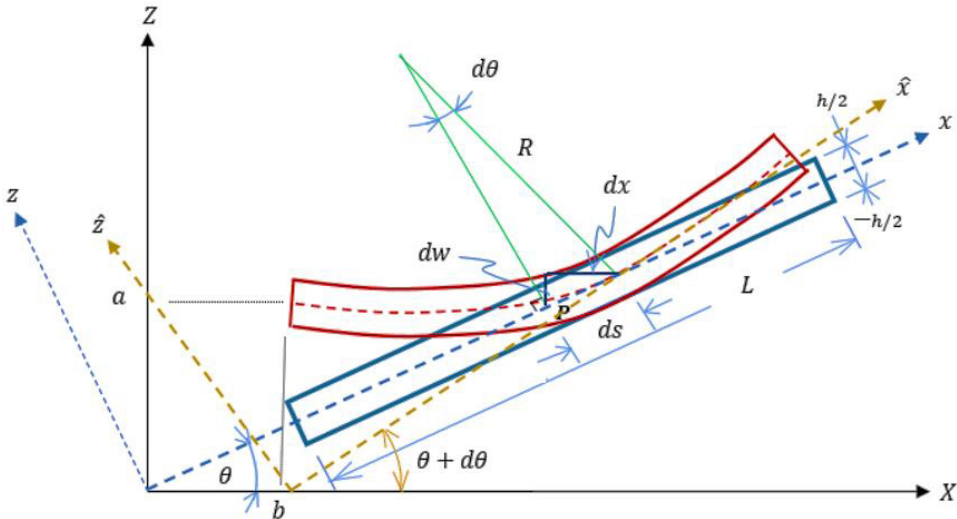


Fig. 1. Undeformed and deformed compliant beam element

The beam element is deformed in the x - z plane that gives rise to the relation in Eq. (1)

$$\frac{1}{R} = \frac{M}{EI} = -\frac{\partial^2 w}{\partial x^2} \left(1 + \left(\frac{\partial w}{\partial x} \right)^2 \right)^{-3/2}, \quad (1)$$

where w is the transverse displacement of the beam, R is the radius of curvature of the beam, EI is the flexural rigidity of the beam, M is the bending moment perpendicular to the axis of bending, dx , dw and ds form a right-angled triangle. ds is a very small portion on the centroid of the deformed beam element. L is the length of the beam element.

Generally, compliant members undergo large deflections, which introduce geometric nonlinearity. For small deformation, the quantity in parenthesis then to unity, reducing Eq. (1) to a mere linear equation in the form, $-\partial^2 w / \partial x^2$. The nonlinear curvature-moment equation in Eq. (1) is used in the derivation of the nonlinear equation governing the large deformation of a compliant beam member. By employing Eq. (1), the kinetic energy, T , the potential energy due to internal force, W_{int} and work done by external force, W_{ext} on the compliant member could be written as:

$$T = \frac{1}{2} \int_0^L \rho A \left(\frac{\partial w}{\partial t} \right)^2 dx, \quad (2)$$

$$W_{int} = -\frac{1}{2} \int_0^L EI \left(\frac{\partial^2 w}{\partial x^2} \right)^2 \left(1 + \left(\frac{\partial w}{\partial x} \right)^2 \right) dx, \quad (3)$$

$$W_{ext} = \frac{1}{2} \int_0^L q w dx \quad (4)$$

giving the Lagrangian, \mathcal{Q} as;

$$\begin{aligned} \mathcal{Q} &= \frac{1}{2} \rho A \left(\frac{\partial w}{\partial t} \right)^2 - \frac{1}{2} EI \left(\frac{\partial^2 w}{\partial x^2} \right)^2 \left(1 + \left(\frac{\partial w}{\partial x} \right)^2 \right) + q w \\ &= \frac{\rho A}{2} \dot{w}^2 - \frac{1}{2} EI w_{xx}^2 (1 + w_x^2) + q w. \end{aligned} \quad (5)$$

The corresponding Euler-Lagrange equation is given as Eq. (6).

$$\frac{\partial \mathcal{Q}}{\partial w} - \frac{\partial}{\partial t} \left(\frac{\partial \mathcal{Q}}{\partial \dot{w}} \right) + \frac{\partial^2}{\partial x^2} \left(\frac{\partial \mathcal{Q}}{\partial w_{xx}} \right) = 0. \quad (6)$$

As such, Eq. (5) transforms into Eq. (7),

$$EI \frac{\partial^4 w}{\partial x^4} \left(1 + \left(\frac{\partial w}{\partial x} \right)^2 \right) + EI \frac{\partial^2 w}{\partial x^2} \left(\frac{\partial^2 w}{\partial x^2} \right)^2 + 4EI \frac{\partial w}{\partial x} \frac{\partial^2 w}{\partial x^2} \frac{\partial^3 w}{\partial x^3} + \rho A \frac{\partial^2 w}{\partial t^2} = q, \quad (7)$$

where ρ and A are the density and cross-sectional area of the beam given by $\pi D^2/4$; D is the diameter of the circular end. Eq. (7) will be the bases for analysis the static and dynamic behaviour of the compliant beam undergoing finite deformation. The non-dimesionalised form of Eq. (7) is given by

$$\frac{\partial^4 \tilde{w}}{\partial \tilde{x}^4} + \frac{\partial^4 \tilde{w}}{\partial \tilde{x}^4} \left(\frac{\partial \tilde{w}}{\partial \tilde{x}} \right)^2 + \frac{\partial^2 \tilde{w}}{\partial \tilde{x}^2} \left(\frac{\partial^2 \tilde{w}}{\partial \tilde{x}^2} \right)^2 + 4 \frac{\partial \tilde{w}}{\partial \tilde{x}} \frac{\partial^2 \tilde{w}}{\partial \tilde{x}^2} \frac{\partial^3 \tilde{w}}{\partial \tilde{x}^3} + \tilde{\rho} \frac{\partial^2 \tilde{w}}{\partial \tilde{t}^2} = \tilde{q}, \quad (8)$$

where

$$\tilde{w} = \frac{w}{L}; \quad \tilde{x} = \frac{x}{L}; \quad \tilde{t} = \frac{t}{L^2} \sqrt{\frac{EI}{\rho A}}; \quad \tilde{\rho} = \frac{\rho AL^3}{EI}; \quad \tilde{q} = \frac{qL^3}{EI}. \quad (9)$$

3. The equation of motion through space function

To separate the transverse displacement function into temporal and spatial components, we adopt the Galerkin's decomposition technique, viz:

$$w(\bar{x}, \bar{t}) = \xi(\bar{x}) \Omega(\bar{t}), \quad (10)$$

where $\Omega(\bar{t})$ the system's generalised coordinate with trial function $\xi(\bar{x})$ that will satisfy Neumann and Dirichlet boundary conditions. On the application of a one-parameter solution to Eq. (8) results to Eq. (11)

$$\int_0^1 \mathfrak{R}(\bar{x}, \bar{t}) \xi(\bar{x}) dx. \quad (11)$$

Here,

$$\mathfrak{R}(\bar{x}, \bar{t}) = \left(\frac{\partial^4 w}{\partial x^4} + \frac{\partial^4 w}{\partial x^4} \left(\frac{\partial w}{\partial x} \right)^2 + \frac{\partial^2 w}{\partial x^2} \left(\frac{\partial^2 w}{\partial x^2} \right)^2 + 4 \frac{\partial w}{\partial x} \frac{\partial^2 w}{\partial x^2} \frac{\partial^3 w}{\partial x^3} + \tilde{\rho} \frac{\partial^2 w}{\partial t^2} - \tilde{q} \right). \quad (12)$$

The equation of motion for the fluid conveying beam could now be derived thus;

$$M \ddot{\Omega}(\bar{t}) + K \Omega(\bar{t}) + N \Omega^3(\bar{t}) + q = 0, \quad (13)$$

where

$$\begin{aligned} M &= \int_0^1 \tilde{\rho} \xi(\tilde{x}) \xi(\tilde{x}) d\tilde{x}, \\ K &= \int_0^1 \xi(\tilde{x}) \frac{d^4 \xi(\tilde{x})}{d\tilde{x}^4} d\tilde{x} \\ N &= \int_0^1 \xi(\tilde{x}) \left(\frac{d^4 \xi(\tilde{x})}{d\tilde{x}^4} \left(\frac{d^2 \xi(\tilde{x})}{d\tilde{x}^2} \right)^2 + \frac{d^2 \xi(\tilde{x})}{d\tilde{x}^2} \left(\frac{d^2 \xi(\tilde{x})}{d\tilde{x}^2} \right)^2 + 4 \frac{d\xi(\tilde{x})}{d\tilde{x}} \frac{d^2 \xi(\tilde{x})}{d\tilde{x}^2} \frac{d^3 \xi(\tilde{x})}{d\tilde{x}^3} \right) d\tilde{x}, \\ q &= - \int_0^1 \xi(\tilde{x}) \tilde{q} d\tilde{x}. \end{aligned} \quad (14)$$

To evaluate the values of M , K , N , and \tilde{q} we will employ a fourth-order polynomial function of the form of Eq. (15) to approximate the trial function, $\xi(\tilde{x}, \bar{t})$

$$\xi(\tilde{x}, \bar{t}) = \eta_0 + \eta_1 \tilde{x} + \eta_2 \tilde{x}^2 + \eta_3 \tilde{x}^3 + \eta_4 \tilde{x}^4 \quad (15)$$

which after the application of the boundary conditions, vis-a-viz; $\xi(0, \bar{t}) = \xi'(0, \bar{t}) = 0$ and $\xi(1, \bar{t}) = \xi'(1, \bar{t}) = 0$ for clamped-clamped beam yields

$$\eta_4 = 3\sqrt{70} / \left((70\mu^4 - 315\mu^3 + 540\mu^2 - 420\mu + 126) \mu^5 \right)^{1/2}. \quad (16)$$

Upon the application of the orthogonality function as $\mu \rightarrow 1$, the value of η_4 becomes $3\sqrt{70}$, making the trial function to be re-defined in the form of Eq. (17)

$$\xi(\tilde{x}, \bar{t}) = \eta_4 (\tilde{x}^2 - 2\tilde{x}^3 + \tilde{x}^4). \quad (17)$$

In the same way, the value of η_4 for a beam that is pinned at both ends with the following boundary conditions, $\xi(0, \bar{t}) = \xi''(0, \bar{t}) = 0$ and $\xi(1, \bar{t}) = \xi''(1, \bar{t}) = 0$ is $3\sqrt{70}/31$, resulting in a new trial function of the form of Eq. (18)

$$\xi(\tilde{x}, \tilde{t}) = \eta_4 (\tilde{x} - 2\tilde{x}^3 + \tilde{x}^4). \quad (18)$$

Also, for a cantilever beam with boundary conditions $\xi(0, \bar{t}) = \xi'(0, \bar{t}) = 0$ and $\xi''(1, \bar{t}) = \xi'''(1, \bar{t}) = 0$, η_4 is $\sqrt{45}/104$ and

$$\xi(\tilde{x}, \tilde{t}) = \eta_4 \left(\frac{3}{8}\tilde{x}^2 - \frac{\tilde{x}^3}{4} + \frac{\tilde{x}^4}{16} \right). \quad (19)$$

4. Basic concept of the multi-step Differential Transformation Method

Let $[0, t]$ be the interval over which we want to find the solution of the initial value problem, which can be approximated, by a DTM finite series solution of the form,

$$y(\tau) = \sum_{k=0}^n f_k \tau^k, \quad \tau \in [0, \tau_1] \quad (20)$$

which is the differential inverse transformation of the differential transformation k -th derivative of $y(\tau)$ defined by

$$Y(k) = \frac{1}{k!} \left(\frac{d^k y(\tau)}{d\tau^k} \right)_{\tau=\tau_0}, \quad \forall \tau \in D, \quad (21)$$

where $Y(k)$ is the transformed function of the original function, $y(\tau)$. The interval $[0, t]$ can be subdivided into n intervals namely $[\tau_{j-2}, \tau_{j-1}, \tau_j]$, for $j = 1, 2, 3, \dots, m$. The equivalent step size is $h = t/m$ with nodes $\tau_i = i h$. The extension of this process to a multi-step phase is based on the following approximate [39],

$$y_1(t) = \sum_{k=0}^n f_{1k} \tau^k, \quad \tau \in [0, \tau_1] \quad (22)$$

with the initial conditions $y_1^{(k)} = c_k$. The initial conditions $y_1^{(k)}(\tau_{j-1}) = y_{j-1}^{(k)}(\tau_{j-1})$ will be used at each subinterval $[\tau_{j-1}, \tau_j]$ through the application of DTM; here, the τ_0 in Eq. (21) will be replaced by τ_{j-1} . The entire process is repeated up to $j = 1, 2, 3, \dots, n$ as sequence of approximation solutions $y_j(\tau)$ are generated at each process. The solution, $y_j(t)$ is now written as,

$$y_j(t) = \sum_{k=0}^n f_{jk} (\tau - \tau_{j-1})^k, \quad \tau \in [\tau_{j-1}, \tau_j] \quad (23)$$

which can be rewritten in piecewise form as,

$$y(t) = \begin{cases} y_1(\tau), & \tau \in [0, \tau_1], \\ y_2(\tau), & \tau \in [\tau_1, \tau_2], \\ y_3(\tau), & \tau \in [\tau_2, \tau_3], \\ \vdots & \vdots \\ y_m(\tau), & \tau \in [\tau_{m-1}, \tau_m]. \end{cases} \quad (24)$$

5. Quasi-static solution of the nonlinear compliant beam

By applying the differential transform theorems [40] on Eq. (8) and neglecting terms in time function, we have the following transformation;

$$\begin{aligned} & \bar{w}(k+4) \frac{(k+4)!}{k!} + \\ & \left(\sum_{r=0}^k \sum_t^{k-r} \left((r+1)(t+1)(k-r-t+4)(k-r-t+3)(k-r-t+2) \right) \right) \\ & \left((k-r-t+1)\bar{w}(r+1)\bar{w}(t+1)\bar{w}(k-r-t+4) \right) \\ & + \sum_{r=0}^k \sum_t^{k-r} \left((r+2)(r+1)(t+2)(k-r-t+2)(k-r-t+1) \right) \\ & \left(\bar{w}(r+2)\bar{w}(t+2)\bar{w}(k-r-t+2) \right) \\ & + \sum_{r=0}^k \sum_t^{k-r} \left((r+2)(r+1)(t+1)(k-r-t+3)(k-r-t+2) \right) \\ & \left((k-r-t+1)\bar{w}(r+2)\bar{w}(t+1)\bar{w}(k-r-t+3) \right) \quad (25) \\ & = \bar{q}(\delta) \end{aligned}$$

which forms the basis of our quasi-static analysis. Equally, the respective boundary conditions are transformed as follows;

(i) double clamped boundary;

$$\bar{w}(0)|_{x=0} = \bar{w}(1)|_{x=0} = 0; \quad \sum_{k=0}^{\infty} \bar{w}(k) \Big|_{x=1} = \sum_{k=0}^{\infty} k \bar{w}(k) \Big|_{x=1} = 0; \quad (26)$$

(ii) double pinned boundary;

$$\bar{w}(0)|_{x=0} = \bar{w}(2)|_{x=0} = 0; \quad \sum_{k=0}^{\infty} \bar{w}(k) \Big|_{x=1} = \sum_{k=0}^{\infty} k \bar{w}(k-1) \Big|_{x=1} = 0; \quad (27)$$

(iii) cantilever;

$$\bar{w}(0)|_{x=0} = \bar{w}(1)|_{x=0} = 0; \quad \sum_{k=0}^{\infty} k \bar{w}(k-1) \Big|_{x=1} = \sum_{k=0}^{\infty} k \bar{w}(k-1)(k-2) \Big|_{x=1} = 0. \quad (28)$$

6. Application of the MsDTM to the Temporal Equation of Motion

By applying the MsDTM to Eq. (8), the following recursive equation could be achieved for $r = 0, 1, 2, \dots, n$.

$$\left(\begin{array}{l} ((r+2)(r+1)\tilde{\Omega}(r+2) + \tilde{k}\tilde{\Omega}(r)) \\ + \tilde{n} \sum_{s=0}^k \sum_{l=0}^m (\tilde{\Omega}(l)\tilde{\Omega}(m-l)\tilde{\Omega}(k-s)) \end{array} \right) = \tilde{q}\delta(r) \quad (29)$$

subject to the transformed initial conditions,

$$\begin{aligned} \tilde{\Omega}_0(0) &= 0, & \tilde{\Omega}_0(1) &= 0 \\ \tilde{\Omega}_j(0) &= \Omega_{j-1}, & \tilde{\Omega}_j(1) &= \Omega'_{j-1}(\tau_j), \quad j = 1, 2, 3, \dots, r \leq m \end{aligned} \quad (30)$$

where, $\tilde{\Omega}$ is the differential transform of Ω , $\tilde{k} = K/M$, and $\tilde{n} = N/M$. Through the resulting recursive equation from Eq. (29), we can generate the corresponding value of $\tilde{\Omega}(r)$. Here, $0 \leq r \leq n$. n represents the number of terms before the truncation of the series. Then, the approximate analytical solution is given in the form of a piecewise power series expansion.

7. Results and discussion

The multi-step differential transformation method (MsDTM) is applied to the temporal nonlinear governing differential equation of motion of a deformed compliant beam, and results show that for various boundary forces and moments, acceptable deformation levels are recorded. It is of interest also to observe that the path of the exact solution and that of the MsDTM results are coinciding favourably as shown by Fig. 2, and the Runge-Kutta numerical scheme in as demonstrated by Figs. 9 through 11. These near-perfect agreement has validated our claims.

As demonstrated in Fig. 2, a family of beam deformation characteristics against its position along the axis is presented. It is clear that sagging increases with increasing values of excitation \hat{q} . The parabolas are found to exhibit minimum values of deformation at the mid-point of the beam, suggesting that the beam is homogeneous when deformation is minimal, and the ends supports are identical. Symmetry about the mid-point of the beam is exhibited. In Fig. 3, it is shown that the large deformation of beam against the axial position (or length) shifts the minimum sagging positions of the family of parabolas away from symmetric points (i.e. $\hat{x} = 0.5$) to around $\hat{x} = 0.7$ for the beam with clamped-clamped ends. This explains the effects of nonlinear components of the system. To demonstrate the influence of large deformation, compliant beam with both large and small deformation considerations are plotted on the same graph. The superimposed plot of the deformation along the dimensionless compliant beam axis with large and

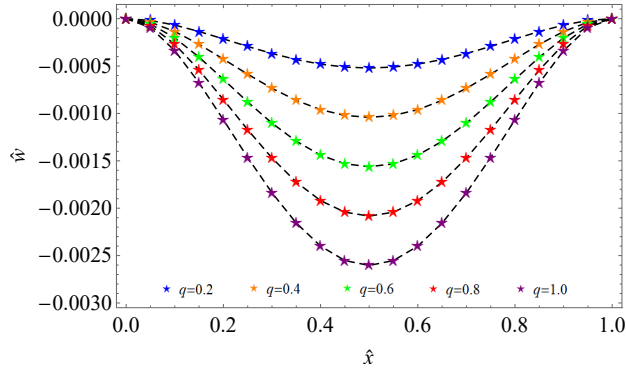


Fig. 2. Deformation along the dimensionless linear Euler-Bernoulli beam axis with small deformation for different load values. The plot markers (*) are for exact solution, while the dashed lines (---) are from the DTM solution. They perfectly agree

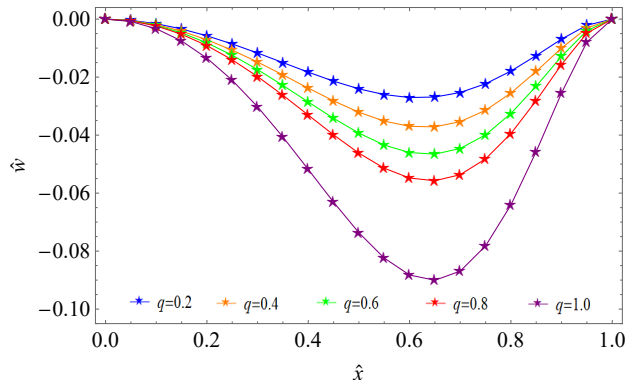


Fig. 3. Deformation along the dimensionless nonlinear Euler-Bernoulli beam axis with large deformation at different load values for a clamped-clamped boundary condition

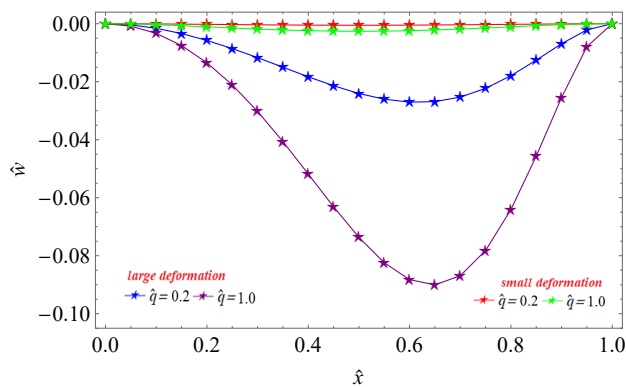


Fig. 4. Superimposed plot of deformation along the dimensionless nonlinear Euler-Bernoulli beam axis with large and small deformations at two load values ($\hat{q} = 0.2$; $\hat{q} = 1.0$) for a clamped-clamped boundary condition

small deformations at two load values ($\hat{q} = 0.2$; $\hat{q} = 1.0$) is shown in Fig. 4. The result reveals that there is a wide range in the values of deflection between the large and small deformation consideration.

Similar effects are reflected in Fig. 5 when the beam is pinned-pinned ended, and deformation becomes large. The family of curves are parabolic with small values of excitation loads applied. However, with increased loadings, it tends to be cubical. In the two cases with similar end conditions, it is expected that the characteristics become symmetric about the mid-point of the beam; however, as a result of the nonlinearity on the system. The cantilevered beam deformation characteristics, as shown in Fig. 6, display a family of curves demonstrating flutters expected of the system. It is shown that as the pipe length increases the slope also increases towards the free end, and as the excitation loads increase the deformation increases.

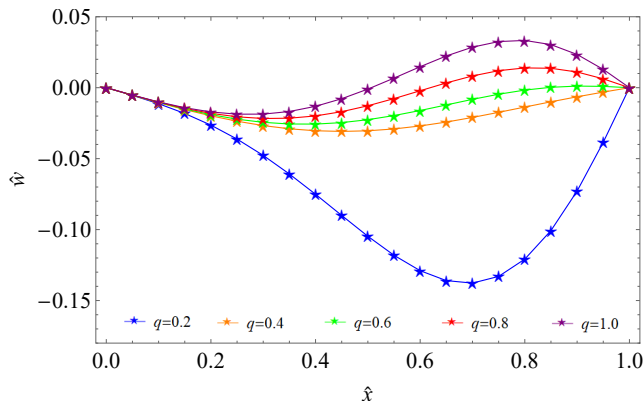


Fig. 5. Deformation along the dimensionless nonlinear Euler-Bernoulli beam axis with large deformation at different load values for a pinned-pinned boundary condition

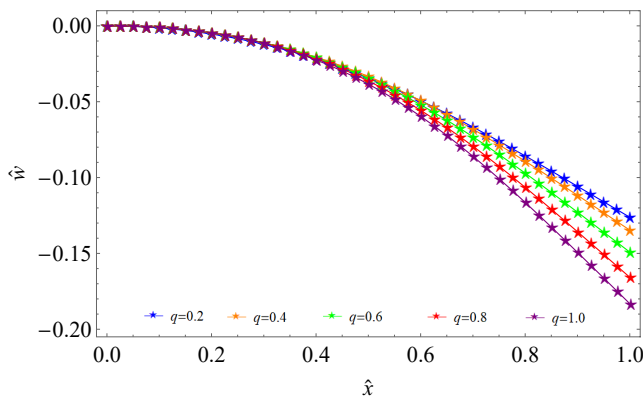


Fig. 6. Deformation along the dimensionless nonlinear Euler-Bernoulli beam axis with large deformation at different load values for a cantilever beam

In Figs. 7 through 9, results of beam deformation against the excitation loads at various positions along the pipe length and different boundary conditions, are presented. As depicted by Fig. 7 compression increases as the load increases for a pipe clamped at both ends. Deformation profile increases in magnitude as the beam position moves to mid-section with a negative slope. For the pinned-pinned boundary conditions, as shown in Fig. 8, the result of deformation against the load is a family of parabolic curves with their turning points being the same at different locations along the pipe length. However, as the load increases deformation decreases in magnitude and as the position at which measurements are taken tends to the mid-section of the beam, the slope of curves become steeper. Fig. 9 illustrates flatter compressive deformation characteristics as the excitation load increases beyond $\hat{q} = 0.2$, although below that value deformation magnitude increases sharply as the load increases between $0 < \hat{q} < 0.2$.

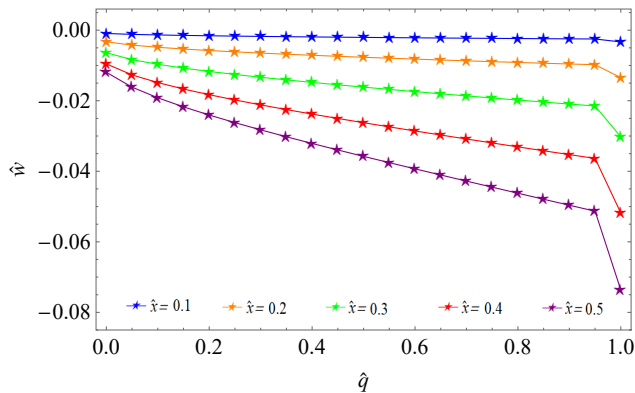


Fig. 7. Deformation of the beam at different dimensionless beam axis positions for a clamped-clamped boundary condition

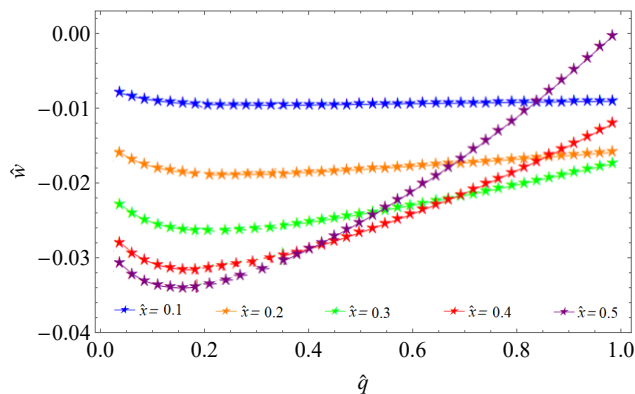


Fig. 8. Deformation of the beam at different dimensionless beam axis positions for a pinned-pinned boundary condition

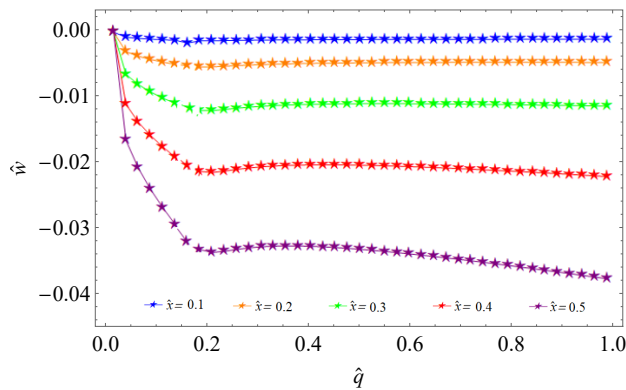


Fig. 9. Deformation of the beam at different dimensionless beam axis positions for a cantilever beam

The demonstration of the system's time history characteristics are presented in Figs. 10 through 11, where the family of harmonics produced with different masses per unit length of pipe illustrates a phase shift of zero in the cases. This shows that the phase shift is increasing linearly with frequency of the harmonic motion. Therefore, in each figure as depicted for both ends clamped (Fig. 10), both ends pinned (Fig. 11) and a cantilever beam (Fig. 12), increasing the mass densities per unit length causes increase in the frequencies of the system.

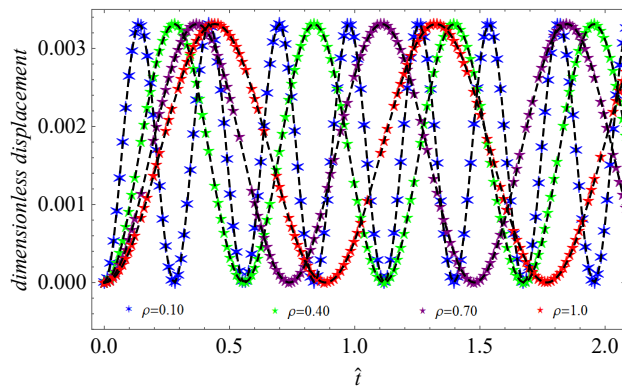


Fig. 10. Time history of the dimensionless displacement at different values of the dimensionless mass per unit length when the beam is clamped at both ends. The plot markers (*) are for RK4, while the dashed lines (- - -) are from the MsDTM solution. They perfectly agree

The time history of velocity at different values of mass per unit length for the is illustrated to be harmonics in Figs. 13–15. The beam when clamped at both ends, as in Fig. 13, reveals a decrease in amplitude as the mass density per unit length increases; however, they are all in-phase with one another because the phase shift is proportional to the frequency. Similarly, in Fig. 14, velocity harmonics are in phase, and as the mass density per unit length increases, the amplitude decreases and the frequency increases. The velocity at different values of mass

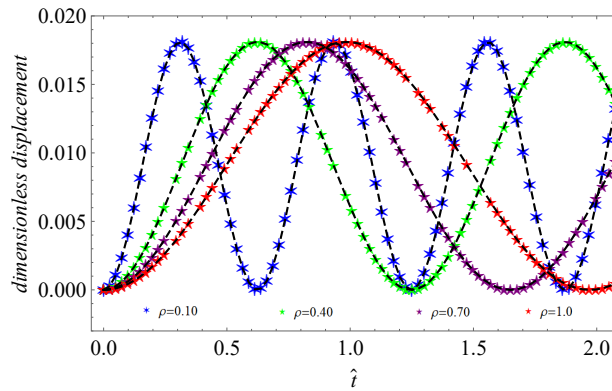


Fig. 11. Time history of the dimensionless displacement at different values of the dimensionless mass per unit length when the beam is pinned at both ends. The plot markers (*) are for RK4, while the dashed lines (- - -) are from the MsDTM solution. They perfectly agree

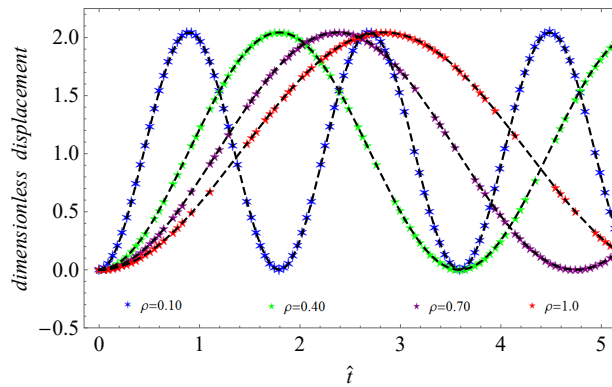


Fig. 12. Time history of the dimensionless displacement at different values of the dimensionless mass per unit length when the beam is a cantilever. The plot markers (*) are for RK4, while the dashed lines (- - -) are from the MsDTM solution. They perfectly agree

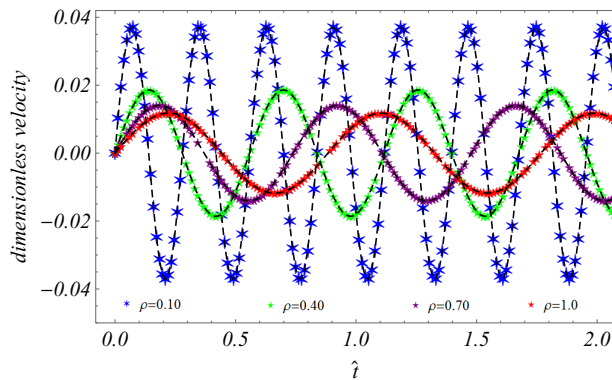


Fig. 13. Time history of the dimensionless velocity at different values of the dimensionless mass per unit length when the beam is clamped at both ends

per unit length for the cantilever beam is demonstrated in Fig. 15. The harmonics show an appreciable increase in frequencies as the mass densities increases, just as demonstrated by Fig. 14, but the amplitudes for the cantilever are much higher than those of a pinned-pinned beam and in those cases higher than for the clamped-clamped beam.

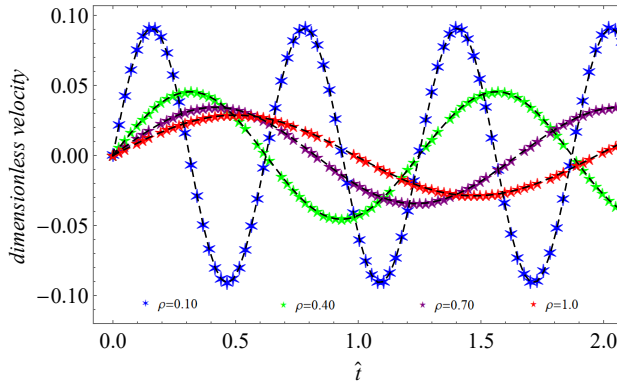


Fig. 14. Time history of the dimensionless velocity at different values of the dimensionless mass per unit length when the beam is pinned at both ends

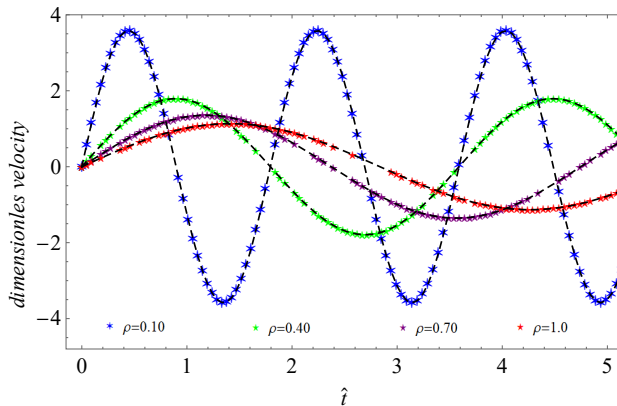


Fig. 15. Time history of the dimensionless velocity at different values of the dimensionless mass per unit length when the beam is a cantilever

The time history of the dimensionless acceleration at different values of the dimensionless mass per unit length is determined with Figs. 16 through 18. For the clamped-clamped beam, the family of curves are harmonics (Fig. 16). It is observed that acceleration decreases with increase in mass density per unit length. As the mass density increases, the lagging phase shift occurs. The amplitude falls, and the frequency increases. Fig. 17 demonstrates acceleration characteristics for a pinned-pinned beam, which gives the harmonic family of curves similar to that of a clamped-clamped system except that amplitude is a little higher in value as for

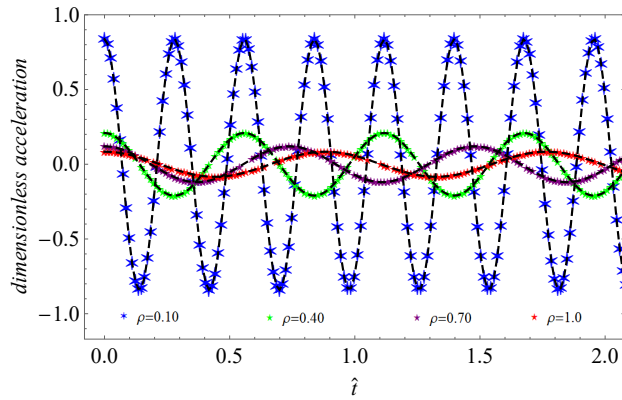


Fig. 16. Time history of the dimensionless acceleration at different values of the dimensionless mass per unit length when the beam is clamped at both ends

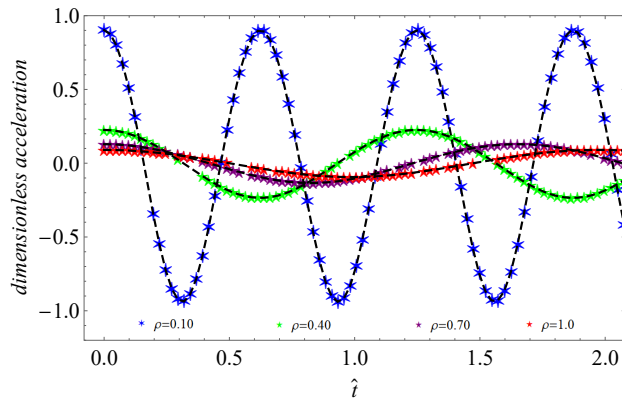


Fig. 17. Time history of the dimensionless acceleration at different values of the dimensionless mass per unit length when the beam is pinned at both ends

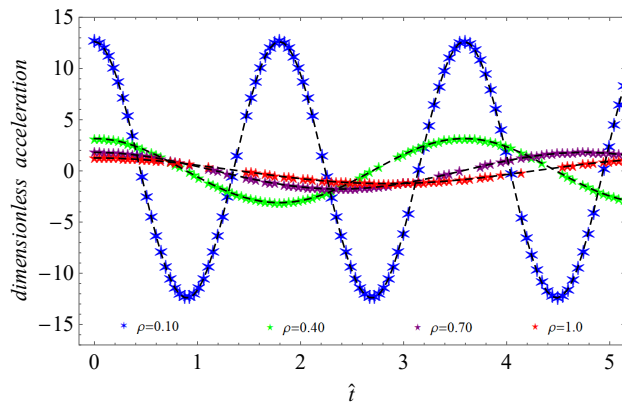


Fig. 18. Time history of the dimensionless acceleration at different values of the dimensionless mass per unit length when the beam is a cantilever

the cantilever, shown in Fig. 18, the family of harmonic curves is demonstrating a zero phase shift, which is a result of the free and clamped ends. A much higher amplitude has resulted in this case, and as the mass density increases, the amplitude falls and the frequency increases.

8. Conclusion

The dynamic model that considers the large deflection of compliant mechanisms has been presented. The geometric nonlinearities due to curvature are taken into account in the formation of the governing equation. The resulting nonlinear partial differential equations do not have closed-form solutions. Consequently, a semi-analytical approach is employed to solve the equation. To subdue the difficulty of capturing the periodic behaviour over a very large region of the solution, MsDTM is used in the solution algorithm. The MsDTM has demonstrated its robustness in handling problems in nonlinear mechanics.

Results have shown that linear analyses for a compliant beam might be deceitful as the behaviour of such systems is extremely nonlinear. The effect of nonlinearity resulting from curvature is of critical importance to this end. This further buttress why compliant systems that are subjected to large deflection may still be nonlinear even with materially linear and homogeneous components.

Parametric studies with variations in beam mass and the excitation load provide a deeper understanding of the behaviour of flexible beam under large deformation.

Manuscript received by Editorial Board, August 26, 2020;
final version, November 23, 2020.

References

- [1] L.L. Howell, S.P. Magleby, and B.M. Olsen. *Handbook of Compliant Mechanisms*. Wiley, 2013. doi: [10.1002/9781118516485](https://doi.org/10.1002/9781118516485).
- [2] K.E. Bisshopp and D.C. Drucker. Large deflection of cantilever beams. *Quarterly of Applied Mathematics*, 3(3):272–275, 1945. doi: [10.1090/qam/13360](https://doi.org/10.1090/qam/13360).
- [3] T.M. Wang. Nonlinear bending of beams with concentrated loads. *Journal of the Franklin Institute*, 285(5):386–390, 1968. doi: [10.1016/0016-0032\(68\)90486-9](https://doi.org/10.1016/0016-0032(68)90486-9).
- [4] T.M. Wang. Non-linear bending of beams with uniformly distributed loads. *International Journal of Non-Linear Mechanics*, 4(4):389–395, 1969. doi: [10.1016/0020-7462\(69\)90034-1](https://doi.org/10.1016/0020-7462(69)90034-1).
- [5] I.S. Sokolnikoff and R.D. Specht. *Mathematical Theory of Elasticity*. McGraw-Hill, New York, 1956.
- [6] R. Frisch-Fay. *Flexible bars*. Butterworths, 1962.
- [7] S.P. Timoshenko and J.M. Gere. *Theory of Elastic Stability*. Courier Corporation, 2009.
- [8] L.L. Howell. *Compliant Mechanisms*. Wiley, New York, 2001.
- [9] T. Beléndez, C. Neipp, and A. Beléndez. Large and small deflections of a cantilever beam. *European Journal of Physics*, 23(3):371–379, 2002. doi: [10.1088/0143-0807/23/3/317](https://doi.org/10.1088/0143-0807/23/3/317).
- [10] T. Beléndez, M. Pérez-Polo, C. Neipp, and A. Beléndez. Numerical and experimental analysis of large deflections of cantilever beams under a combined load. *Physica Scripta*, 2005(T118):61–64. 2005. doi: [10.1238/Physica.Topical.118a00061](https://doi.org/10.1238/Physica.Topical.118a00061).

- [11] K. Mattiasson. Numerical results from large deflection beam and frame problems analysed by means of elliptic integrals. *Iterational Journal for Numerical Methods in Engineering*, 17(1):145–153, 1981. doi: [10.1002/nme.1620170113](https://doi.org/10.1002/nme.1620170113).
- [12] F. De Bona and S. Zelenika. A generalised elastica-type approach to the analysis of large displacements of spring-strips. *Proceedings of the Institution of Mechanical Engineers, Part C: Journal of Mechanical Engineering Science*, 211(7):509–517, 1997. doi: [10.1243/0954406971521890](https://doi.org/10.1243/0954406971521890).
- [13] H.-J. Su. A pseudorigid-body 3R model for determining large deflection of cantilever beams subject to tip loads. *Journal of Mechanisms and Robotics*, 1(2):021008, 2009. doi: [10.1115/1.3046148](https://doi.org/10.1115/1.3046148).
- [14] H. Tari, G.L. Kinzel, and D.A. Mendelsohn. Cartesian and piecewise parametric large deflection solutions of tip point loaded Euler–Bernoulli cantilever beams. *International Journal of Mechanical Sciences*, 100:216–225, 2015. doi: [10.1016/j.ijmecsci.2015.06.024](https://doi.org/10.1016/j.ijmecsci.2015.06.024).
- [15] Y.V. Zakharov and K.G. Okhotkin. Nonlinear bending of thin elastic rods. *Journal of Applied Mechanics and Technical Physics*, 43(5):739–744, 2002. doi: [10.1023/A:1019800205519](https://doi.org/10.1023/A:1019800205519).
- [16] M. Batista. Analytical treatment of equilibrium configurations of cantilever under terminal loads using Jacobi elliptical functions. *International Journal of Solids and Structures*, 51(13):2308–2326, 2014. doi: [10.1016/j.ijsolstr.2014.02.036](https://doi.org/10.1016/j.ijsolstr.2014.02.036).
- [17] R. Kumar, L.S. Ramachandra, and D. Roy. Techniques based on genetic algorithms for large deflection analysis of beams. *Sadhana*, 29(6):589–604, 2004.
- [18] M. Dado and S. Al-Sadder. A new technique for large deflection analysis of non-prismatic cantilever beams. *Mechanics Research Communications*, 32(6):692–703, 2005. doi: [10.1016/j.mechrescom.2005.01.004](https://doi.org/10.1016/j.mechrescom.2005.01.004).
- [19] B.S. Shvartsman. Large deflections of a cantilever beam subjected to a follower force. *Journal of Sound and Vibration*, 304(3-5):969–973, 2007. doi: [10.1016/j.jsv.2007.03.010](https://doi.org/10.1016/j.jsv.2007.03.010).
- [20] M. Mutyalarao, D. Bharathi, and B.N. Rao. On the uniqueness of large deflections of a uniform cantilever beam under a tip-concentrated rotational load. *International Journal of Non-Linear Mechanics*, 45(4):433–441, 2010. doi: [10.1016/j.ijnonlinmec.2009.12.015](https://doi.org/10.1016/j.ijnonlinmec.2009.12.015).
- [21] M.A. Rahman, M.T. Siddiqui, and M.A. Kowser. Design and non-linear analysis of a parabolic leaf spring. *Journal of Mechanical Engineering*, 37:47–51, 2007. doi: [10.3329/jme.v37i0.819](https://doi.org/10.3329/jme.v37i0.819).
- [22] D.K. Roy and K.N. Saha. Nonlinear analysis of leaf springs of functionally graded materials. *Procedia Engineering*, 51:538–543, 2013. doi: [10.1016/j.proeng.2013.01.076](https://doi.org/10.1016/j.proeng.2013.01.076).
- [23] A. Banerjee, B. Bhattacharya, and A.K. Mallik. Large deflection of cantilever beams with geometric nonlinearity: Analytical and numerical approaches. *International Journal of Non-Linear Mechanics*, 43(5):366–376, Jun. 2008. doi: [10.1016/j.ijnonlinmec.2007.12.020](https://doi.org/10.1016/j.ijnonlinmec.2007.12.020).
- [24] L. Chen. An integral approach for large deflection cantilever beams. *International Journal of Non-Linear Mechanics*, 45(3)301–305, 2010. doi: [10.1016/j.ijnonlinmec.2009.12.004](https://doi.org/10.1016/j.ijnonlinmec.2009.12.004).
- [25] C.A. Almeida, J.C.R. Albino, I.F.M. Menezes, and G.H. Paulino. Geometric nonlinear analyses of functionally graded beams using a tailored Lagrangian formulation. *Mechanics Research Communications*, 38(8):553–559, 2011. doi: [10.1016/j.mechrescom.2011.07.006](https://doi.org/10.1016/j.mechrescom.2011.07.006).
- [26] M. Sitar, F. Kosel, and M. Brojan. Large deflections of nonlinearly elastic functionally graded composite beams. *Archives of Civil and Mechanical Engineering*, 14(4):700–709, 2014., doi: [10.1016/j.acme.2013.11.007](https://doi.org/10.1016/j.acme.2013.11.007).
- [27] D.K. Nguyen. Large displacement behaviour of tapered cantilever Euler–Bernoulli beams made of functionally graded material. *Applied Mathematics and Computation*, 237:340–355, 2014. doi: [10.1016/j.amc.2014.03.104](https://doi.org/10.1016/j.amc.2014.03.104).
- [28] S. Ghuku and K.N. Saha. A theoretical and experimental study on geometric nonlinearity of initially curved cantilever beams. *Engineering Science and Technology, an International Journal*, 19(1):135–146, 2016. doi: [10.1016/j.jestch.2015.07.006](https://doi.org/10.1016/j.jestch.2015.07.006).

- [29] A.M. Tarantino, L. Lanzoni, and F.O. Falope. *The Bending Theory of Fully Nonlinear Beams*. Springer, Cham, 2019. doi: [10.1007/978-3-030-14676-4](https://doi.org/10.1007/978-3-030-14676-4)
- [30] S.J. Salami. Large deflection geometrically nonlinear bending of sandwich beams with flexible core and nanocomposite face sheets reinforced by nonuniformly distributed graphene platelets. *Journal of Sandwich Structures & Materials*, 22(3):866–895, 2020. doi: [10.1177/1099636219896070](https://doi.org/10.1177/1099636219896070).
- [31] T.T. Akano. An explicit solution to continuum compliant cantilever beam problem with various variational iteration algorithms. *Advanced Engineering Forum*, 32:1–13, 2019. doi: [10.4028/www.scientific.net/aeef.32.1](https://doi.org/10.4028/www.scientific.net/aeef.32.1).
- [32] J.K. Zhou. *Differential Transformation and its Applications for Electrical Circuits*. Huazhong University Press, Wuhan, China, 1986.
- [33] S.K. Jena and S. Chakraverty. Differential quadrature and differential transformation methods in buckling analysis of nanobeams. *Curved and Layered Structures*, 6(1):68–76, 2019. doi: [10.1515/cls-2019-0006](https://doi.org/10.1515/cls-2019-0006).
- [34] M. Kumar, G.J. Reddy, N.N. Kumar, and O A. Bég. Application of differential transform method to unsteady free convective heat transfer of a couple stress fluid over a stretching sheet. *Heat Transfer – Asian Research*, 48(2):582–600, 2019. doi: [10.1002/htj.21396](https://doi.org/10.1002/htj.21396).
- [35] G.C. Shit and S. Mukherjee. Differential transform method for unsteady magnetohydrodynamic nanofluid flow in the presence of thermal radiation. *Journal of Nanofluids*, 8(5):998–1009, 2019. doi: [10.1166/jon.2019.1643](https://doi.org/10.1166/jon.2019.1643).
- [36] D. Nazari and S. Shahmorad. Application of the fractional differential transform method to fractional-order integro-differential equations with nonlocal boundary conditions. *Journal of Computational and Applied Mathematics*, 234(3):883–891, Jun. 2010. doi: [10.1016/j.cam.2010.01.053](https://doi.org/10.1016/j.cam.2010.01.053).
- [37] M.A. Rashidifar and A.A. Rashidifar. Analysis of vibration of a pipeline supported on elastic soil using differential transform method. *American Journal of Mechanical Engineering*, 1(4):96–102, 2013. doi: [10.12691/ajme-1-4-4](https://doi.org/10.12691/ajme-1-4-4).
- [38] Y. Xiao. Large deflection of tip loaded beam with differential transformation method. *Advanced Materials Research*, 250-253:1232–1235, 2011. doi: [10.4028/www.scientific.net/AMR.250-253.1232](https://doi.org/10.4028/www.scientific.net/AMR.250-253.1232).
- [39] Z.M. Odibat, C. Bertelle, M.A. Aziz-Alaoui, and G.H.E. Duchamp. A multi-step differential transform method and application to non-chaotic or chaotic systems. *Computers & Mathematics with Applications*, 59(4):1462–1472, 2010. doi: [10.1016/j.camwa.2009.11.005](https://doi.org/10.1016/j.camwa.2009.11.005).
- [40] A. Arikoglu and I. Ozkol. Solution of differential-difference equations by using differential transform method. *Applied Mathematics and Computation*, 181(1):153–162, 2006. doi: [10.1016/j.amc.2006.01.022](https://doi.org/10.1016/j.amc.2006.01.022).